# Influence of Microstructure on the Fracture Toughness of Tungsten Alloys

B. Gludovatz[1,2], M. Faleschini[2], S. Wurster[2], A. Hoffmann[3], R. Pippan[1,2]

[1]CD Laboratory for Local Analysis of Deformation and Fracture, Jahnstr. 12; Leoben, Styria, 8700, Austria
[2]Erich Schmid Institute of Materials Science, Austrian Academy of Sciences, Jahnstr. 12; Leoben, Styria, 8700, Austria
[3]Plansee Metall GmbH; Reutte, Tyrol, 6600, Austria

Keywords: tungsten, tungsten alloys, fracture toughness, electron backscatter diffraction, auger-electron spectroscopy, inter- and transcrystalline fracture

## Abstract

Tungsten and tungsten alloys show the typical change in fracture behaviour from brittle at low temperatures to ductile at high temperatures. In order to improve the understanding of the effect of microstructure the fracture toughness of pure tungsten, potassium doped tungsten and tungsten with 1wt% $La_2O_3$ has been investigated by means of 3-point bending -, double cantilever beam - and compact tension specimens. All these materials show the expected increase in fracture toughness with increasing temperature. The experiments show that the grain size, texture, chemical composition, grain boundary segregation and dislocation density seem to have a large effect on fracture toughness below the DBTT. These influences can be seen in the fracture behaviour and morphology, where two kinds of fracture occur: on one hand the transcrystalline and on the other hand the intercrystalline fracture. Therefore techniques like electron backscatter diffraction, auger electron spectroscopy and x-ray line profile analysis were used to improve the understanding of the parameter influencing fracture toughness.

## Introduction

Most studies related to the ductility of tungsten and tungsten alloys have been performed in the sixties and seventies (e.g. Raffo et al. [1]). Since fracture mechanics was not well established at that time the studies on fracture toughness were scarce. In the nineties Riedle and Gumbsch [2, 3] studied extensively the fracture toughness of tungsten single crystals. The effect of crystallographic orientation, crack growing direction, loading rate and temperature has been investigated. In contrary, the fracture toughness of polycrystalline tungsten is not well examined.

We have started an extensive investigation of the fracture toughness of pure tungsten (W), potassium doped tungsten (AKS-W) and tungsten with 1wt% $La_2O_3$ (WL10). The results of few selected microstructures are presented in this paper. A very large effect of the microstructure especially below the ductile to brittle transition temperature has been observed. The investigation seems to indicate that the change from transcrystalline to intercrystalline cleavage fracture plays an important role. Fractographic as well as crystallographic analysis are presented to improve the understanding of interaction of these fracture processes.

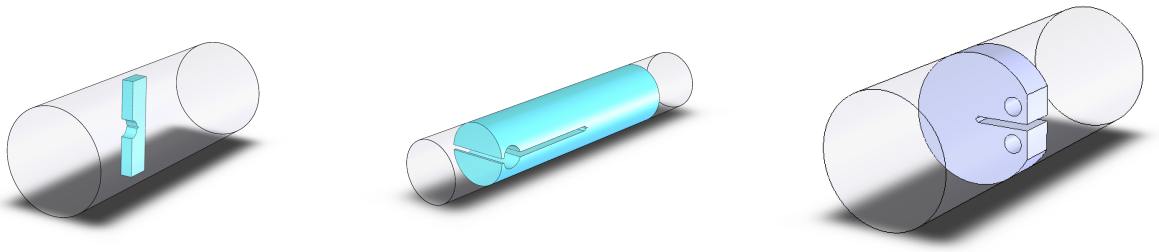

(a) 3PB-specimen (b) DCB-specimen (c) CT-specimen

Figure 1: Different specimen types manufactured out of tungsten rods. 3PB-specimen with crack direction in rolling direction (a). DCB-specimen with crack direction in rolling direction (b). CT-specimen with crack direction in tangential direction (c).

## Experimental

W, AKS-W and WL10 have been investigated by means of 3-point bending - (3PB - fig.1-a), double cantilever beam - (DCB - fig.1-b) and compact tension specimens (CT - fig.1-c). All specimens were manufactered out of rods during different stages of the processing route. Figure 1 shows specimens for tests in rolling - (RD) and tangential direction (TD) additional ones have been prepared for tests in normal direction (ND). Especially AKS-W has been studied to investigate the longitudinal splitting of the AKS-W wires, the crack propagation direction with the lowest fracture toughness. Tests were performed in the range of -196°C to more than 1000°C. To get an idea of the influence of the grain structure electron backscatter diffraction (EBSD) analysis of the wires at different diameters between the center and the edge of the AKS-W wires have been carried out by use of a Zeiss 1525 scanning electron microscope equipped with an EDAX EBSD system.
Additional discs with a diameter of 6mm and height of approximately 0.6mm were produced from W, AKS-W and WL10. After the manufacturing process the discs were deformed at 400°C ($\approx 0.17\ T_m$) by high pressure torsion under a constant pressure of 8GPa. The discs were processed at a relative low rotational speed of 0.2 rotations per minute which corresponds to a strain rate of roughly $\dot{\varepsilon}$=$2min^{-1}$ and were performed to a maximum equivalent strain of $\varepsilon$=256 at to a radius of 2mm.
Furthermore a DCB-specimen with a length of 30mm, a height of 3mm and a width of 5mm was prepared with a notch and a pre-crack. This specimen was tested in-situ in the SEM by cleaving the cantilever. After breaking the specimen the obtained EBSD scans and the SE and BSE images of the fracture surface are use to to quantify the fracture process.

## Results and Discussion

### Fracture Toughness Investigations

All tested specimens showed an increase in fracture toughness with increasing temperature, an example is shown in figure 2-a. At low temperatures the fracture toughness was determined in standard experiments whereas at temperatures above 600°C the critical crack tip opening displacement [4] was used to determine the critical stress intensity factor. The

Table 1: $K_{IC}$ values of W and W alloys tested at different specimens at room temperature

| Material | Condition | Rod diameter / mm | Tests performed | $K_{IC}$ / MPa$\sqrt{m}$ |
|---|---|---|---|---|
| W | as sintered | 23 | CT | 5.1 |
| | rolled | 9 | CT | 4.69 |
| | forged | 25 | 3PB | 8.01 |
| | rolled | 9 | 3PB | 9.08 |
| | rolled | 4 | 3PB | 5.43 |
| | rolled and drawn | 1 | 3PB | 35.09 |
| WL | as sintered | 23 | CT | 4.72 |
| | rolled | 9 | CT | 5.99 |
| | forged | 25 | 3PB | 16.56 |
| | rolled | 9 | 3PB | 9.77 |
| | rolled | 4 | 3PB | 9.74 |
| AKS-W | as sintered | 23 | CT | 6.45 |
| | rolled | 9 | CT | 4.50 |
| | rolled | 9 | 3PB | 32.07 |
| | rolled | 4 | 3PB | 13.48 |
| | rolled and drawn | 1 | 3PB | 32.06 |
| WRe (25%) | forged | 25 | 3PB | 54.24 |

fracture toughness is given by

$$K_{IC} = \sqrt{m \cdot \sigma_y \cdot E \cdot COD_C} \tag{1}$$

where $\sigma_y$ represents the yield strength, $E$ the Young's modulus and $m$ a coefficient which depends on the work hardening factor $n$ of the material. For low hardening $n$ is approximately $\approx 0.5$ [5]. Table 1 shows fracture toughness values of CT and 3PB specimens tested at room temperature. Due to the extreme range of the determined $K_{IC}$ values the processing route seems to have a great influence on the results as well as the direction the specimens have been manufactured out of the rods. Additionally it has to be mentioned that different specimens from the same wires show sometimes large differents. For example 3PB-specimens from the center of an AKS-W wire give much lower $K_{IC}$ values than DCB-specimens where the crack propagated through the whole cross section. Therefore small 3PB-specimens over the whole cross-section were manufactured and tested. Figure 2-b shows the results in the different positions AKS-W wires. Starting from extremely low values in the center of the wire the fracture toughness increases when reaching half of the radius. At the edge of the wire the values again decrease. The EBSD scans show a change in the texture as a function of the radius. The pronounced $\langle 1\,1\,0 \rangle$ texture in the center changes to a $\langle 1\,0\,0 \rangle$ texture at half of the radius of the rod whereas at the edge $\langle 1\,1\,0 \rangle$ texture dominates again. This change in texture fits very well to the obtained variation of the fracture toughness values.

Ultra-fine Grained W-Alloys [6]

From table 1 it seems to be evident that a refinement of the microstructure with decreasing wire diameter appears to increase the fracture toughness. Therefore the effect of severe deformation which can be used to refine the microstructure was investigated. Figure 3-a is showing the microstructure of highly deformed W at a true strain of $\varepsilon$=256. The evolution of the structural size during HPT-deformation can be seen in figure 3-b for tungsten and potassium doped tungsten. The higher the deformation, the higher the misorientation of

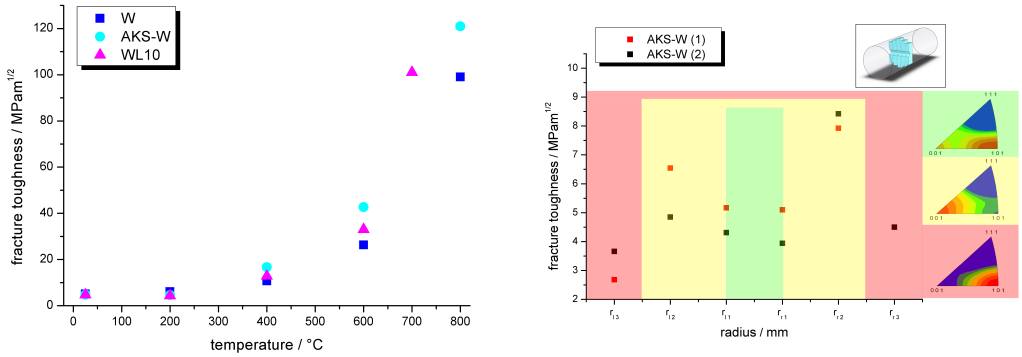


(a) Fracture toughness $K_{IC}$ versus temperature $T$ of sintered CT-specimens.

(b) Local fracture toughness of AKS-W tested at room temperature.

Figure 2: $K_{IC}$ of sintered W, AKS-W and WL10 as a function of $T$ (a). The local fracture toughness of $\langle 1\,1\,0 \rangle$ oriented grains seems to be much lower than of $\langle 1\,0\,0 \rangle$ oriented grains (b).

the grains and the more pronounced the grain refinement. It's noticeable that above a true strain of approximately $\varepsilon$=32 no further grain refinement takes place and saturation seems to occur. The thermal stability of these microstructures was studied by annealing in vacuum at 800°C, 1000°C and 1200°C for 1 hour. While pure tungsten started to recrystallize at 800°C the potassium doped tungsten did not show a significant increase in grain size until 1200°C. Figure 4-a shows the steady grown grains of pure tungsten and 4-b the somewhat coarsened microstructure of AKS-W after 1 hour at 1200°C respectively. In both materials annihilation of dislocations and recrystallization started at lower temperatures than 1200°C, however the taken BSE images of the microstructures demonstrated the much higher thermal stability of AKS-W after high pressure torsion deformation. The influence of a thermal treatment on the microstructure and therefore the fracture behaviour and fracture toughness of pure tungsten is well known. Due to recrystallization starting at 800°C of severely deformed pure tungsten we can expect the fracture toughness to drop after such a treatment. The determined $K_{IC}$ values of SPD deformed tungsten and the heat treated SPD samples are presented in figure 5-a, 5-b shows the variation of fracture toughness versus the yield strength

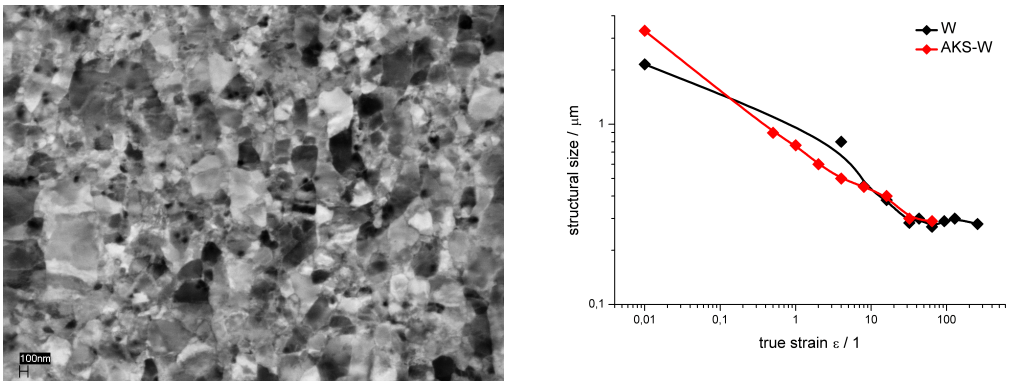


(a) BSE image of microstructure of SPD-W at $\varepsilon$=256

(b) Structural size in dependence of applied strain for W and AKS-W

Figure 3: The higher the applied strain, the higher the grain refinement until a value of $\varepsilon$=32 where saturation is reached.

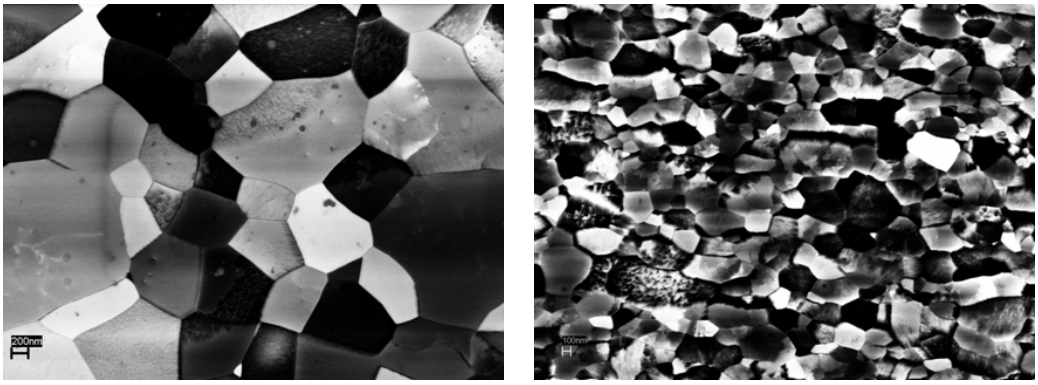

(a) Microstructure of SPD-W ($\varepsilon$=32) (b) Microstructure of SPD-AKS-W ($\varepsilon$=32)

Figure 4: Evolution of microstructure of SPD-W (a) and SPD-AKS-W (b) after a thermal treatment at 1200°C. Both materials have been heavy deformed to $\varepsilon$=32.

for few selected W and heat treated SPD-AKS-W samples. The grain refinement induces a significant increase in the fracture toughness as well as the yield strength. Annealing of AKS-W at 800°C and 1000°C causes a small decrease in yield strength, however it does not affect the toughness. Annealing at 1200°C induces a further decrease of yield stress however a significant reduction in the fracture toughness.
Grain refinement usually causes an increase in ductility however such large increase has not been expected. Increase in crack deflection and reduction in grain boundary impurities due to the increase in grain boundary area may be the reason for this pronounced improvement in toughness. However by SPD the increase of toughness as well the decrease by annealing is not well understood and requires further investigations.

## Intercrystalline vs. transcrystalline crack growth

In order to understand better the effect of intercrystalline and transcrystalline crack growth the pre-cracked DCB specimen was tested in-situ at the SEM. The crack path could be recorded by the EBSD system as well as by taking some SE images and some BSE images

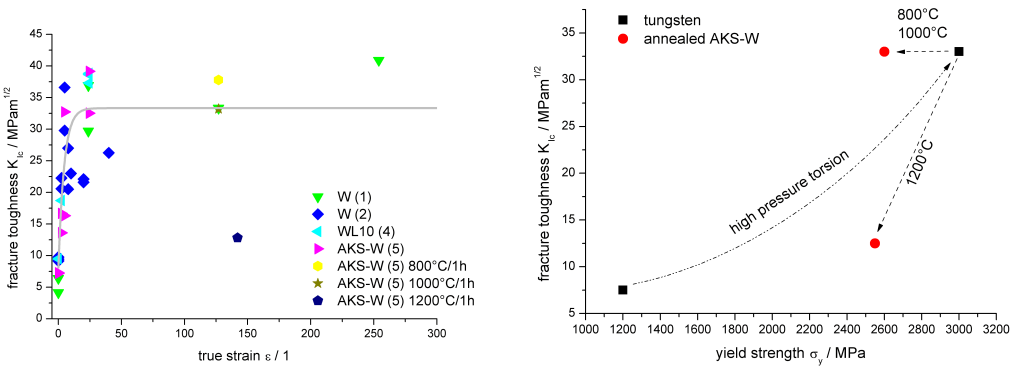


(a) Fracture toughness of SPD-W alloys as a function of the applied strain and the effect of annealing in SPD deformed AKS-W.

(b) Fracture toughness $K_{IC}$ vs. $\sigma_y$ of W and AKS-W before/after HPT and heat treated SPD-AKS-W.

Figure 5: Fracture toughness of severely deformed tungsten alloys and the effect of annealing in severely deformed AKS-W.

after breaking the sample. The analyse shows two types of fracture behavior (figure 6), on one hand the crack propagates intercrystalline (ik) and on the other hand also transcrystalline (tk). Measurements along the intercrystalline part of the crack path show a completely random distribution of misorientations of cleaved neighboring grains between 20 degrees and 60 degrees. In the case of intercrystalline crack propagation not only grain boundaries, sometimes also subgrain boundaries are cleaved. This experiments show that crystallographic quantification of fracture process is possible.
In order to quantify this effect of intercrystalline cleavage fracture of grain and subgrain boundaries and the transcrystalline cleavage fracture further investigations on different microstructures (grain size, grain microstructure, grain boundary impurities, etc.) will be performed and described in a forthcoming paper.

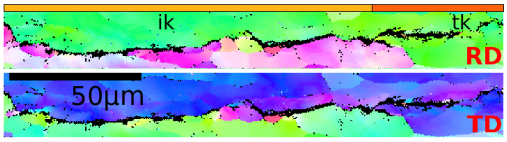


(a) EBSD scan of AKS-W in RD/TD.

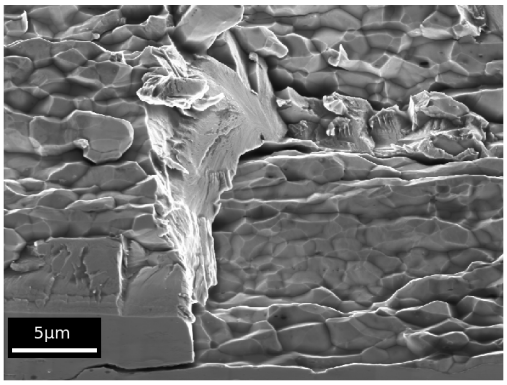


(b) SE image of AKS-W. The specimen was tilted at 45°.

Figure 6: AKS-W with a crack in rolling direction. The EBSD scan (a) is showing the ik and the tk fracture behavior as well as the SE image (b).

## References


[1] P.L. Raffo. Yielding and fracture in tungsten and tungsten-rhenium alloys. *Journal of the Less Common Metals*, 17:133–149, 1969.

[2] J. Riedle. *Bruchwiderstand in Wolfram-Einkristallen: Einfluss der kristallographischen Orientierung, der Temperatur und der Lastrate*, volume 18: Mechanik/Bruchmechanik. VDI Verlag, 1990.

[3] P. Gumbsch. Modeling and simulation in materials science. *Summer School of Fracture, Udine (lecture notes)*, 2005.

[4] O. Kolednik and H.P. Stüwe. The stereophotogrammetric determination of the critical crack tip opening displacement. *Engineering Fracture Mechanics*, 21:145–155, 1985.

[5] O. Kolednik and H.P. Stüwe. A proposal for estimating the slope of the blunting line. *International Journal of Fracture*, 33:R63–R66, 1987.

[6] M. Faleschini, H. Kreuzer, D. Kiener, and R. Pippan. Fracture toughness investigations of tungsten alloys and SPD tungsten alloys. *Journal of Nuclear Materials*, 367-370:800–805, 2007.